醫工學會誌 : 第10卷, 第 2 號, 1989
J. of KOSOMBE : Vol. 10, No. 2

研 究 論 文
89- 2 -03

인공심장용 전동기구동형 혈액 펌프의 설계 및 해석에 관한 연구

천 길 정 · 김 희 찬 · 민 병 구 · 한 동 철*

Design and Analysis of A New Type of the Motor-Driven Blood Pump for Artificial Heart

Gill J. Cheon, Hee C. Kim, Byoung G. Min, Dong C. Han*

—Abstract—

A new motor-driven blood pump for artificial heart was developed. In this blood pump, a small size, high torque brushless DC motor was used as an energy converter and the motor rolls back and forth on a circular track. This movement of the "rolling-cyliner" causes blood ejection by alternately pushing left or right polyurethane blood sacs. This moving-actuator mechanism could be eliminate two potential problems of other motor-driven artificial hearts such as large size and poor anastomosis for the implantation. Theoretical analyses on the pump efficiency, the temperature rise, and the inflow mechanism were also performed. In a series of mock circulation tests, the theoretical analyses were compared to the measured hemodynamic and mechanical values. The pump system was shown to have sufficient cardiac output (upto 9 L / min), sensitivity to preload, and mechanical stability to be tested as an implantable total artificial heart.

요 점

새로운 형태의 인공심장용 전동기구동형 혈액 펌프를 개발하였다. 개발된 혈액 펌프는 소형, 고출력, 브러쉬 없는 직류 전동기를 에너지 변환 장치로 사용하였으며, 이 전동기 자체가 원호 형태의 궤적을 따라 좌우로 회전하도록 고안되었으며, 전동기를 포함한 '회전원통'의 움직임이 좌우에 부착되어 있는 폴리우레탄으로 제작된 혈액 주머니를 번갈아 밀게 되어 혈액을 박출하게 된다.

본 연구에서 도입한 이동형 작동기 원리에 의해 다른 전동기 구동형 혈액 펌프가 안고 있는 두가지의 중요한 문제점인 펌프 크기의 증가와 자연 심장과의 해부학적인 구조상 접합의 문제점들을 개선할 수 있었다. 또한 펌프의 효율과 전동기에 의한 시스템의 온도 상승, 그리고 펌프 내에 유입되는 유체에 대한 이론적 해석을 실시하였으며, 일련의 모의 순환 실험을 통해 실험 결과를 비교하였다.

개발된 펌프 시스템은 이식형 완전 인공 심장으로 사용하기에 충분한 심박출량(9 L / m)과 전부하에 민감한 반응, 그리고 기계적인 안정도를 보여 주었다.

< 접수: 1989년 6월22일 >

서울대학교 의과대학 의공학교실 ·
서울대학교 공과대학 기계설계학과*
Department of Biomedical Engineering, College of Medicine, and Department of Mechanical Design and Production Engineering, College of Engineering*, Seoul National University

Introduction

Since the first permanent artificial heart was implanted inside the human chest[1], a series of blood pumps for artificial heart have been developed[2~5]. They can be categorized into the se-

veral groups depending upon the type of energy souce, energy converter, and pump actuator.

Although the pneumatically driven devices have achieved some successs in human implantation, these systems are not suitable for long-term implantation due to the large bore percutaneous tubes and the lack of portability of the driving unit.

Electrical motor driven blood pumps have advantages due to its possibility of the tether-free totally implantable artificial heart using subcutaneous rechageable battery and transcutaneous energy transmission (TET) device. But most existing motor driven blood pumps also have major disadvantages of large size and fitting problem for clinical application.

In the autors' laboratory, the new type motor driven blood pump for artificial heart has been developed since 1984 with the following two design objectives. The first is to reduce the total size of the pump to be implanted into the relatively small thoracic cavity of women and Orientals. The second objective is to provide a high compatibility in fitting blood pump to the remnant of the natural atria and arterial vessels.

The basic idea of our new blood pump is to eliminate the dead space occupied by the energy converter by rolling the motor back and forth to produce blood ejection. Thus, our system can be called as "moving-actuator" or "rolling-cylinder" mechanism.

In addition to the pump size reduction, by rolling the actuator on a circular track, the interdistance between the right and left inflow ports is considerably reduced and the outflow ports' orientations are crossed each other with a sufficient angle for easy fitting to arteries. This factor is very important in surgical procedure[6]. In most motor-driven artificial heart system, the inflow ports are located far apart and the right and left outflow ports are in parallel direction each other. Then, these long and straight orientations of aortic and pulmonary arterial grafts are very poor for anatomosis and vulnerable to kinking of graft.

Since the implantable battery and TET system's capacities are limited, the pump efficency is one of the most important factors to realize the totally implantable artificial heart system[7]. The total sytem efficiency is also related to thermal problems, reliability of the system, and local hot spots in the pump. The build-up of the pressure in the interspace between two ventricles is also very critical problem during diastolic blood filling, as it can cause the reduced cardiac output. In this paper, theoretical analyses on these three factors were also performed and the results of analysis were verified in the mock circulation experiments.

Materials and Methods

Descriptions of Blood Pump

The new blood pump consists of three major parts: right and left ventricles and pump actuator including a motor as an energy converter. The artificial ventricle is a polyurethane blood sac. As shown in Fig. 1, the contraction of each

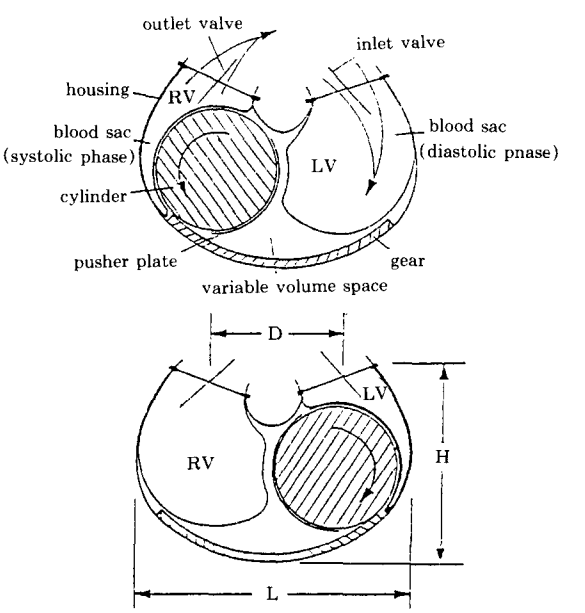

Fig. 1. Schematic diagrams of the rolling-cylinder type blood pump.

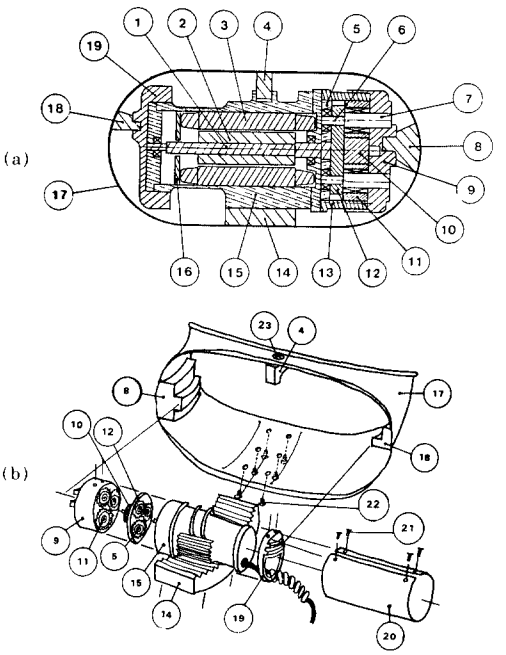

Fig. 2. (a) Structural sketch of the actuator, and (b) Perspective view of the actuator assembly.

ventricle occurs alternately as the motor cylinder rolls back and forth.

The rolling motion of cylinder was produced by the gear and rack mechanism, as shown in Fig. 2. The rotation of the rotor is transferred to the one side end cap of the cylinder through the two stages of planetary gears with the speed reduction of 28:1. The arc-shaped guide bar fixed to the outer actuator frame, prevents this rotational motion of the end cap. Thus, the center part of the cylinder rotates in return while the other side end cap and guide bar ensures this rotational motion by sustaining the cylinder. Then, by the action-reaction principle between the gear engraved at the lower surface of the cylinder and the rack fixed to the actuator frame, the whole cylinder rolls back and forth through a circular track as the rotational direction of the motor changes.

As separated in motion from the center part of the cylinder, the both side end caps provide the translational motion, and then, the pusher plates attached to these end caps alternately contract each blood sac.

A high-torque brushless DC motor with small diameter and long length(S / M 566-18, Sierracin / Magnedyne) was chosen as an energy converter. Determination of the dimensions of all mechanical components and selection of the materials for fabrication were carefully performed to guarantee five years operation without failure. For the purpose of lubrication and heat dissipation, the inner space of blood pump was filled with silicon oil(KF-96-100CS, Shin-Etsu Che-

Table-1. Parts list for mechanical components.

Part	Qts	Description	Material
1	1	Rotor shaft	SCM-4
2	1	Rotor	S / M 566-18
3	1	Stator	S / M 566-18
4	1	Mechanical Brake	Ti-6Al-4V
5	3	lst planetary gears	Ti-6Al-4V
6	3	lst gear shafts	SCM-4
7	3	2nd gear shafts	SCM-4
8	1	Frontal guide bar	S45C
9	1	Frontal end cap	MC Acryl
10	1	2nd sun gear	S45C
11	3	2nd planetary gears	Ti-6Al-4V
12	1	Follower	S45C
13	1	Internal Gear	S45C
14	1	Rack	S45C
15	1	Motor housing with surface engraved gear	Duralumin
16	1	Hall effect sensor board	S / M 566-18
17	1	Actuator frame	Stainless Steel Pl.
18	1	Rear guide bar	S45C
19	1	Rear end cap	MC Acryl
20	1	Pusher plate	Stainless Steel Pl.
21	4	Flat top screws	MSWR10
22	6	Screws	MSWR10
23	1	Screw	MSWR10

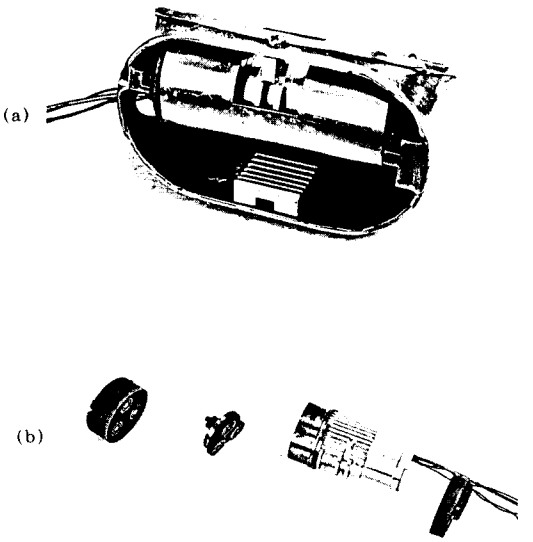

Fig. 3. Pictures of (a) the total actuator assembly, and (b) the rolling-cylinder assembly.

mical Co. Ltd). The parts of mechanical components for pump actuator are summarized in Table 1, and Fig. 3 are the pictures of the fabricated pump actuator. The overall dimensions of the blood pump of Fig. 1 are as follows: pump height(H) is 7cm, interdistance between left and right ports(D) is 4cm, length(L) is 10cm, width (W) is 11cm, and weight is 810 gr.

Theoretical Analysis

1) Pump Efficiency

The efficiency breakdown through the power delivery route from motor to blood sac, and the power loss at each component was established as shown in Fig. 4.

a) Output hydraulic power

The necessary hydraulic pump output power is given by the following equation,

$$\underset{[\text{watt}]}{Ph} = \underset{[\text{mmHg}]}{(\text{afterload} - \text{preload})} \cdot \underset{[\text{mmHg}]}{\text{cardiac output}} \cdot \underset{[\text{L/min}]}{0.00222} \quad (1)$$

$$[\text{watt/mmHg} \cdot \text{L/min}]$$

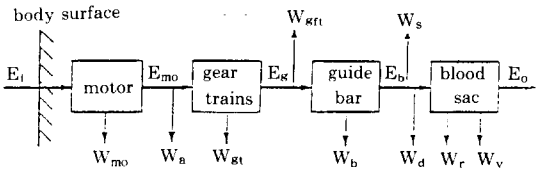

Fig. 4. Diagram of the power delivery route and the possible power loss sites.

Then, if we neglect the preload effect, the output hydraulic powers are 1.95(watt) and 0.44(watt) for left and right blood pump, respectively at the hemodynamic condition of 8 (L/min) of cardiac output, 110 (mmHg) of aortic pressure, and 25 (mmHg) of pulmonary arterial pressure. Since the new blood pump is an alternately ejecting type, the maximum required power output is determined by the left pump.

b) Valvular loss

The prosthetic valve has power loss in the forms of back flow and pressure drop[8]. If we define the efficiency of valve as η_v, the power loss by the valve is given as follows,

$$Wv = \frac{1-\eta_v}{\eta_v} \cdot Ph \quad (2)$$

c) Residual blood volume loss

The remaining blood volume in the ventricle during systolic phase has its internal energy loss as pressure decrease during diastolic phase and it is represented as follows,

$$Wr = Qr \cdot \delta P \quad (3)$$

where Qr is the remaining blood volume and δP is the pressure decease. The amount of th is power loss is negligible compared to the other factors.

d) Drag force loss

When the cylinder moves in oil bath, there exists drag force to resist the movement and the power loss relating to this force is given by,

$$Wd = Fd \cdot V,\ Fd = Cd \cdot \frac{p \cdot V^2 \cdot Acs}{2} \quad (4)$$

Where Fd is drag force, V is the cylinder ve-

locity, Cd is a drag coefficient[9], and Acs is the cylinder surface area, and p is oil density.

e) Squeeze loss

Cylinder movement in oil bath produces another loss component which occurs by the squeezed oil between the cylinder and pump housing wall. This loss is given by,

$$Ws=\frac{p\cdot v^3}{2}\cdot\frac{(Ach\cdot Acc)(Ach+Acc)}{(Ach-Acc)^2} \quad 5)$$

Where Ach and Acc are the cross sectional areas of the housing and cylinder, respectively.

f) Guide bar loss

There exist frictional loss between the guide bar and the end cap with both vertical and horizontal force components. Guide bar efficiency is defined as a function of a friction coefficient between guide bar and end cap materials and cylinder dimensions as follows,

$$\eta b=1-\mu\cdot\frac{D+\mu\cdot Lc}{D} \quad (6)$$

where μ is a friction coefficient between guide bar and end cap materials, and D and Lc are diameter and length of cylinder, respectively.

g) Gear's side face frictional loss

Between the gear face and gear plate in the planetary gear train, there exists relative motion and the resultant total frictional loss due to this relative motion is given by,

$$Wgf=Ng\cdot\frac{\pi}{2}\cdot v\cdot\frac{r^4}{h}\cdot wg^2 \quad (7)$$

Where Ng is total number of gears, v is viscosity of oil, h is oil film thickness, wg is angular velocity, and r is radius of gear.

h) Gear loss

In ideal condition, spur gear efficiency is given as follws[10],

$$\eta g=1-\pi\cdot\mu\cdot\left(\frac{1}{N1}+\frac{1}{N2}\right) \quad (8)$$

Where μ is frictional coefficient of gear material and N1 and N2 are teeth numbers of each stage gear.

i) Motor air gap loss

When the clearance between rotor and stator of motor is filled with oil, there exists frictional power loss as follow,

$$Wa=2\pi v\cdot\frac{r^2\cdot Lr\cdot wr^2}{u} \quad (9)$$

Where v is oil viscosity, Lr is rotor length, u is clearance, and wr is angular velocity.

j) Motor loss

The efficiency of motor is defined as a ratio of mechanical shaft output power to electrical input power. In our case, mechanical output power of motor is determined by the sum of the required hydraulic pump output power and all of loss factors,

$$Po=Ph+\sum(\text{all of loss factors}) \quad (10\text{-a})$$
$$=T\cdot W \quad (10\text{-b})$$

Where T is output torque and W is angular velocity of motor. In this equation, since the angular velocity of motor is determined from the heart rate and the dimensional relationship of mechanical components, the shaft output torque can be obtained. Then, the electrical input power is calculated using the other motor constants as follows,

$$Pi=E\cdot I \quad (11\text{-a})$$
$$=(I\cdot R+Kb\cdot W)\cdot I \quad (11\text{-b})$$
$$=\left(\frac{T}{Kt}\cdot R+Kb\cdot W\right)\cdot\frac{T}{Kt} \quad (11\text{-c})$$

Where E is terminal voltage, I is input current, R is stator resistance, Kb is back emf constant, and Kt is torque constant of motor. Then, the resultant efficiency of motor is given by,

$$\eta m=\frac{Po}{Pi} \quad (12)$$

Table 2 provides theoretical efficency of total system, where it is estimated to be as much as 38(%). We did not include the switching loss of electrical controller circuit in this estimation. As shown is Table 2, the total system efficiency

Table-2 Estimated eficiency breakdown of the developed blood pump at 8(L / min) cardiac output, 110(mmHg) AoP, and 25(mmHg) PAP.

Loss Factor	Loss [Watt]	Input Power [Watt]	Component Efficiency [%]	Output Power [Watt]	System Efficiency [%]
Right Pump	–	–	–	0.44	
Left Pump	–	–	–	1.95	
Valve (Wv)	0.217	2.167	90.0	1.95	
Drag Loss (Wd)	0.013	2.180	99.0	2.167	
Squeeze Loss (Ws)	0.024	2.204	99.0	2.180	
Guide Bar(Wgb)	1.394	3.598	61.3	2.204	
Gear Face (Wg)	0.010	3.608	99.7	3.598	
Gear (Wg)	0.251	3.859	93.5	3.608	
Air Gap(Wa)	0.240	4.099	94.1	3.859	47.4
Motor (Wm)	0.993	5.092	80.5	4.099	38.2

can be represented as the product of efficiencies of two subsystems, motor and remaining mechanical components. In realization of blood pump system, if we allow the fabricational margin of each subsystem by 70(%), then the expected pump efficiency could be at least about 20(%).

2) Thermal Equilibrium

If the pump efficiency is 20(%), the amount of heat generation in the pump is given by,

$$H=(1-{}^{n}\text{pump})/{}^{n}\text{pump}\cdot Ph \qquad (13)$$
$$=7.8(\text{Watt})=1.86(\text{Cal}/\text{sec})$$

This generated heat is transferred through the silicon oil to blood flow and pump housing. Assuming that the all amount of heat is dissipated by blood flow, then temperature increase of blood is calculated as follows,

$$\delta Tb=Tbo-Tbi=\frac{H}{C\cdot Q\cdot P} \qquad (14)$$

Where Tbo, and Tbi are the outflow and inflow blood temperature, respectively, C is the specific heat of blood, Q is flow rate, and p is blood density. It we assume $C\simeq 1$(Cal / g ℃) and use Q=8 (L / min), and p=1.056(g / ml), then the temperature increase is 0.013 (℃) and negligible. Thermal management problems, therefore, depends upon the efficiency of heat transfer from the pump to blood flow.

After thermal equilibrium is reached, the temperature gradient will be formed as shown in Fig. 5, and the temperature distribution is calculated by the following equations[11],

$$H=Hb+Ht \qquad (15\text{-a})$$

$$H=Jo\cdot(As+Ah)\cdot(To-T1) \qquad (15\text{-b})$$

$$Hb=\frac{As\cdot ks}{ds}\cdot(T1-T2) \qquad (15\text{-c})$$

$$=Jb\cdot As\cdot(T2-Tb) \qquad (15\text{-d})$$

$$Ht=\frac{Ah\cdot kh}{dh}\cdot(T1-Ts) \qquad (15\text{-d})$$

Where Hb and Ht are the dissipated heat through blood flow and surrounding tissue, respectively,

Jo and Jb are the convective heat transfer coefficients of oil and blood, respectively,

Ah and As are the area of pump housing and blood sac, respectively,

kh and ks are the thermal conductivity

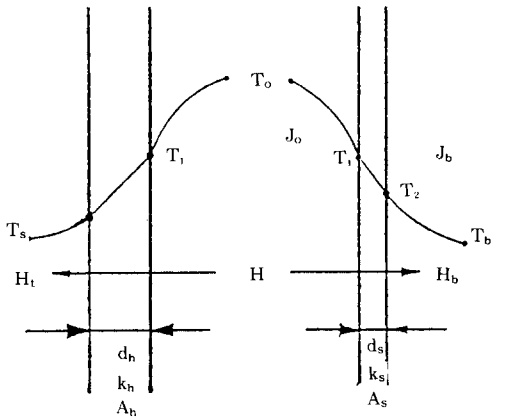

Fig. 5. Temperature gradients between the intermediate oil and the blood and the surrounding tissue

Where Hb and Ht are the dissipated heat through blood flow and surrounding tissue, respectively,

Jo and Jb are the connvective hear transfer coefficients of oil and blood, respectively,

Ah and As are the area of pump housing and blood sac, respectively,

kh and ks are the thermal conductivity of pump housing and blood sac, respectively,

dh and ds are the thickness of pump housing and blood sac, respectively,

Tb and Ts are the temperatures of blood and surrounding tissue, respectively,

To is the temperature of intermediate oil, and

T1 is the temperature of blood sac or pump housing at oil contacting side, and

T2 is the temperature of blood sac at blood contacting side.

of pump housing and blood sac, respectively,

dh and ds are the thickness of pump housing and blood sac, respectively,

Tb and Ts are the temperatures of blood and surrounding tissue, respectively,

To is the temperature of intermediate oil, and

T1 is the temperature of blood sac or pump housing at oil contacting side, and

T2 is the temperature of blood sac at blood contacting side.

Assuming Jo=Jb=500(W / ㎡ ℃), ks=kh=0.05(W / m ℃), and Tb=Ts=36.5(℃), and

using H=6.175(W), Ah=As=120(㎠), ds=0.05(cm), and dh=0.2(cm),

then the calculated temperature values and amount of dissipated heat are as follows,

To=43.15(℃), T1=42.50(℃),
T2=37.50(℃)

Hb=6.0(W), Ht=1.8(W).

Hence, if 1.8(W) and 6.0(W) of heat are dissipated through the surrounding tissue and blood flow, respectively, then no temterature rises in blood and surrounding tissue will be occurred theoretically. Since the intermediate oil keeps contact with the cylinder surface, and the stator of motor is located in touch with this metal cylinder surface, the temperature rise up to the maximum winding temperature of 155(℃) will not occur while the oil temperature is maintained 43.15(℃).

2) Pump Inflow Mechanism

In the artificial heart system, the diastolic filling characteristic is very important to provide sufficient cardiac output sensitive diastolic filling to preload, and to prevent obstruction of venous return. To analyze the pump inflow mechanism, a simple mathewmatical model of the blood pump was used.

If flow through the valve is assumed to be laminar, the inflow rate is given by Poiseulle's law[12],

$$\frac{d}{dt}Q(t)=\frac{1}{Rv}\cdot(Pat-Piv(t)) \qquad (16)$$

Where Q(t) is the inflow volume, Rv is the equivalent resistance of inflow port, Pat is the atrial pressure, and Piv(t) is the intraventricular pressure.

In this equation, since Rv and Pat can be regarded as constants, Piv(t) is the major factor to influence the inflow volume. Unless the ventricular sac is strained, the intraventricular pressure and the interspacial pressure between the right and left ventricles are same. This pressure in the interspace between the two sacs is expressed as follows,

$$\delta Pvv = \frac{-\delta V}{Vo} \cdot \beta eq \qquad (17\text{-a})$$

$$\text{or, } Pvv(t) - Pvv(o) = -\frac{Qa(t) - Q(t)}{Vo} \cdot \beta eq \qquad (17\text{-b})$$

Where Pvv(t) is the interspacial pressure, and Q(t) is the inflow volume of one ventricle, Qa (t) is the outflow volume of the other ventricle, Vo is the initial interspace volume, and βeq is the equivalent bulk modulus[13].

From the equations of (16) and (17), assuming Pvv(0) is zero when the pump housing is completely sealed under the atmospheric pressure, the inflow volume satisfies the following differential equation,

$$\frac{1}{Rv} \cdot \left(Pat + \frac{Qa(t) - Q(t)}{Vo} \cdot Beq\right) = \frac{d}{dt} Q(t) \qquad (18)$$

With the initial condition of Q(0)=0 and the assumption of the linearly increased outflow volume of

$$Qa(t) = mt, \quad 0 \leqq t \leqq T, \qquad (19)$$

equation (18) has the following solution,

$$Q(t) = mt + \frac{Rv \cdot Vo}{\beta eq} \cdot \left(\frac{Pat}{Rv} - m\right) \cdot \left(1 - e^{-\frac{\beta eq \cdot t}{Rv \cdot Vo}}\right) \qquad (20)$$

for $0 \leqq t \leqq T$.

and the interspacial pressure Pvv(t) is given by

$$Pvv(t) = (Pat - m \cdot Rv) \cdot \left(1 - e^{-\frac{\beta eq \cdot t}{Rv \cdot Vo}}\right). \qquad (21)$$

The solution of equation (21) reduces to the following simple forms at the extremity of βeq,

$$\underset{\beta eq=0}{Q(t)} = \frac{Pat}{Rv} \cdot t, \quad 0 \leqq t \leqq T, \qquad (22\text{-a})$$

$$\underset{\beta eq=\infty}{Q(t)} = mt, \quad 0 \leqq t \leqq T, \qquad (22\text{-b})$$

As expected, if βeq equals zero, where the interspace is exposed to the atmosphere, the inflow volume is determined by the atrial pressure and inflow resistance (passive filling case), If βeq has infinite value, for the case of completely hard sealing, the inflow volume of one ventricle depends upon the other sac's outflow volume (active filling case). Since it is almost impossible to make zero βeq in the implantable artificial heart, some investigators connected a variable volume device, or compliance chamber to the interspace to have relatively low βeq. In this case, the inflow volume is significantly limited as the prosthetic blood pump has the increased inflow resistance, Rv, compared to the natural heart. The present analyses results show that the extent of filling can be regulated by the change of flexibility of the pump housing.

Description of Control System

The control system of the blood pump consists of three parts: position control unit, velocity control unit, and power control unit. To provide the position commutation for the brushless DC motor, three Hall effcet sensors are used and activated by the flux of the rotor magnet. As the rotor rotates, they produce sequences of pulses, and these pulses are also used for the position and speed controls as well as the postion commutation.

In the position control unit, the output pulse of the Hall effect sensors are combined and counted. When the output of the counter reaches

to the preset value, the rotational direction of the motor is altered and the counter is reset. This position control scheme provides us a very easy stroke length adjustment method by just changing the preset counter value.

These Hall sensor pulses are also used as input to the frequency-to- voltage converter for the purpose of the motor speed measurement in the velocity control unit. The measured velocity signal is compared to the reference velocity profile and its error signal drives the power control unit through a proportional, integral, and dervative (PID) controller. Total 64 sets of different refererece velocity profiles are stored as a function of position[14] in two erasable programmable read only memory (EPROM) devices. To adjust the diastolic filling time of each ventricle, the left and right diastasis (waiting) time control circuit is also provided. These two control parameters, velocity profile selection and the left and right diastasis time control, can be adjusted by manual or automatic method.

In the power control unit, the pulse width modulation (PWM) method is used using a three phase, full bridge MOSFET (IRF 540, I&R) inverter. The voltage drop across the current sensing resistor is measured for the current limiting as well as the aortic pressure estimation as the load of the motor. The microprocessor system provides automatic control parameter adjustment and monitors the operating state of the pump instantaneously to display the following parameters: heart rate, left to right diastolic filling period ratio, and aortic pressure.

Mock circulation experiments

The pump system was attached to a modified Donovan mock circulation system which hydraulically simulates the systemic and pulmonary circulations[15]. This circulatory system consists of four separated chambers, which represent systemic arterial, systemic venous, pulmonary arterial, and pulmonary venous chambers. All of the chambers are hermatically sealed. A rotameter for volumetric flow rate measurement provide data on the cardiac output, and the four pressure transducers are connected to the chambers to provide pressure data. Also, additional pressure transducer was located inside the pump to monitor the pressure change in the interspace between the two ventricles. The mock circulation system's flowing media was water mixed with glycerin to make the solution viscosity similar to blood. A 8-channel A / D converter connected to a IBM PC / XT personal computer was used to collect the various signals and analyze them.

Results and discussion

A typical waveform of aortic, pulmonary arterial, left atrial, and right atrial pressure in the mock circulation tests is shown in Fig. 6. The response of cardiac output to the physiologic variations is shown in Fig. 7. Cardiac output(C.

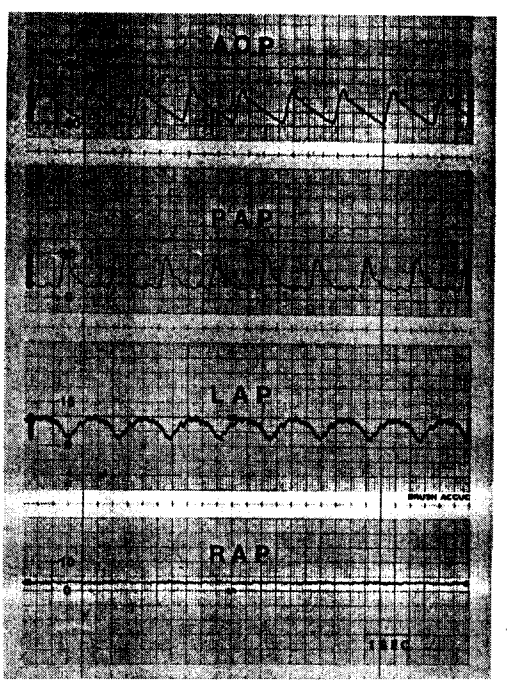

Fig. 6. Typical waveforms of the results of mock circulation experiments: aotic(AoP), pulmonary arterial(PAP), left atrial(LAP), and right atrial(RAP) pressure from the top.

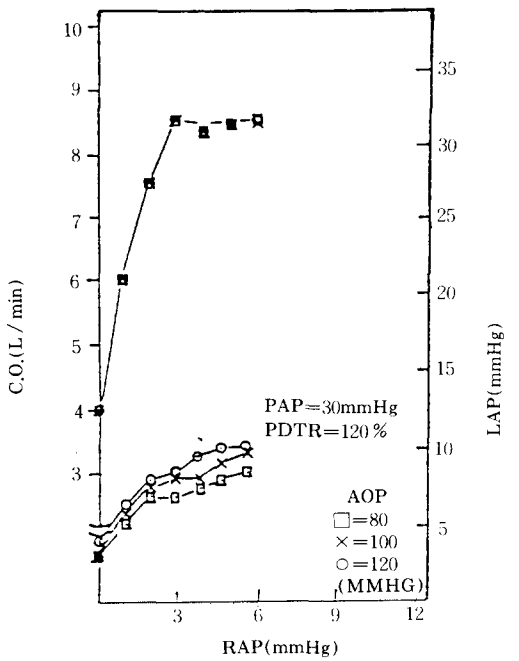

Fig. 7. Cardiac output response to preload and the relationship of left atrial pressure and right atrial pressure.

O.) and left atrial pressure (LAP) are plotted against the right atrial pressure (RAP). With a rise of RAP from 0 to 6(mmHg), the cardiac output increses from 4.5 to 9(L/min)[15], with the heart rate increase from 60 to 120(BPM). These results show the sufficient pump capacity for the necessary blood flow rate of 100(Kg) recipient based upon minimum 80(ml/min/Kg) for survival.

When the cardiac output is 9(L/min) and aortic pressure is 120(mmHg), the require mean input current is 1.2(A) and the mean input voltage is 18(V). The resultant input and output powers are 21.6(W) and 2.38(W), respectively, which indicates that the whole pump efficiency is just about 11(%). The main cause of this large discrepancy between the expected and measured pump efficiency may be the degree of the fabricational and assembeing precision for the mechanical components, especially gears and guide bars. Also, the motor efficiency may be overestimated, as the motor is running in alternating direction with time-varying velocity profile. Also, the various coefficients used in the theoretical analysis may be different from actual values.

Just after the three days of continuous operation, the pump was detached from the mock circulation system and disassembled for temperature measurement. The measured temperature difference between water and motor housing was 17.3(℃), higher by two times of theoretical value of 6.65(℃). Since the temperature rise in blood pump is directly related to the pump efficiency, the overestimated pump efficinecy can cause the underestimated temperature rise. This temperature rise is still within the range of the allowable motor operational temperature.

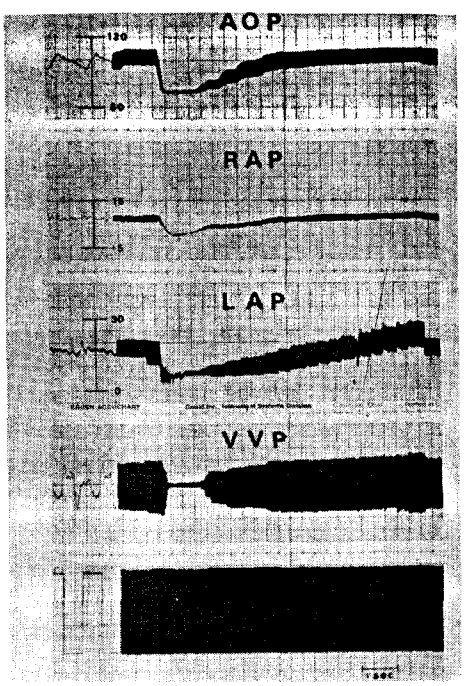

Fig. 8. Waveforms of the interspacial pressure(VVP) change between right and left ventricles according to the increase of left atrial pressure(LAP) together with the changes of AoP, and RAP.

Regarding the inflow mechanism, the pump has both preload sensitivity and mild active filling characteristics using somewhat flexible pump housing. Preload sensitive filling characteristic was confirmed by the interspacial pressure changes caused by variations in LAP and RAP. In Fig. 8, the interspacial pressure is shown to increase together with increase of the atrial pressures. This indicates the preload related filling characteristic. The extent of active filling is shown in Fig. 7 with cardiac output of 4(L / min) at zero level of RAP. These two results may verify our theoretical analysis for inflow mechanism.

In conclusion, the present motor-driven blood pump has structural adventages compared to other motor type and pneumatic blood pumps. Also, it is verified in a series of mock circulation tests that the system has sufficient cardiac output (upto 9 L / min), reliablility, and stability to be tried as a new artifical heart system. Futher efforts to improve the pump efficiency by both mechanical and electrical approachese are still required, as shown by the discrepancdy between the theoretical and measured values.

References

1) Devris, W.C., et al., "Clinical Use of the Total Artificial Heart," N. Eng. J. Med., 310(5), 1984, pp. 273-278.
2) Pierce, W.S., "The Artificial Heart—1986: Partial Fulfillment of a Promise," Trans. Am. Soc. Artif. Intern. Organs, Vol. XXXII, 1986, pp.5-10.
3) Suith, W.A., et al., "The E4T Electric Powered Total Artificial Heart (TAH)," Artificial Organs, 12(5): 1988, pp. 402-409.
4) Nose, Y, "Totally Implantable Artificial Organs: Cardiac Prosthesis," Artificial Organs, 10(2): 1986, pp.102-113.
5) Atsumi, K, "Research and Development on the TAH- from the Engineering Aspects," Artificial Organs, 10(1): 1986, 12-19.
6) Rosenberg, G., et al., "An Electric Motor-driven Total Artificial Heart: Seven Months Survival in the Calf," Trans. Am. Soc. Artif. Intern. Organs, Vol. XXX, 1984, pp. 69-74.
7) Tsach, U., et al., "Minimum Power Consumption of the Electric Ventricular Assist Device Through the Design of an Optimal Output Controller," Trans. Am. Soc. Artif. Intern. Organs, Vol. XXXIII, 1987, pp. 714-719.
8) Gabbay S., et al., "In Vitro Hydrodynamic Comparison of St. Jude, Bjork-Shiley, and Hall-Kaster Valves,"Trans. Am. Soc. Artif. Intern. Organs, Vol. XXVI, 1980.
9) Sabersky, R.H., et al., Fluid Flow, Macmillan Co., 1971.
10) Spott, M.F., Mechanical Design Analysis, Prentice Hall, N.Y., 1964.
11) Holman, J.P., Heat Transfer, McGraw-Hill, 1976.
12) Kamiya, A., et al., "Effects of Unphysiological Factors on Cardiac Output Regulation During Artificial Heart Pumping," IEEE Trans. Biomed. Eng., Vol. BME-22, No. 3, May. 1975, pp.238-245.
13) Merritt, H.E., Hydraulic Control System, John Wiley & Sons, N.Y., 1967.
14) Rosenberg, G., et al., "A Cam-type Electric Motor-driven Left Ventricular Assist Device," Transactions of the ASME, Vol. 104, Aug. 1982, pp.214-220.
15) Lioi, A.P., et al., "In vitro Development of Automatic Control for the Actively Filled Electrohydraulic Heart," Artificial Organs, 12(2): 1988, pp. 152-162.